



## Controls on methane concentration and stable isotope ( $\delta^2\text{H-CH}_4$ and $\delta^{13}\text{C-CH}_4$ ) distributions in the water columns of the Black Sea and Cariaco Basin

J. D. Kessler,<sup>1,2</sup> W. S. Reeburgh,<sup>1</sup> and S. C. Tyler<sup>1</sup>

Received 10 June 2005; revised 6 July 2006; accepted 21 July 2006; published 2 November 2006.

[1] Methane ( $\text{CH}_4$ ) concentration and stable isotope ( $\delta^2\text{H-CH}_4$  and  $\delta^{13}\text{C-CH}_4$ ) depth distributions show large differences in the water columns of the Earth's largest  $\text{CH}_4$ -containing anoxic basins, the Black Sea and Cariaco Basin. In the deep basins, the between-basin stable isotope differences are large, 83‰ for  $\delta^2\text{H-CH}_4$  and 9‰ for  $\delta^{13}\text{C-CH}_4$ , and the distributions are mirror images of one another. The major sink in both basins, anaerobic oxidation of  $\text{CH}_4$ , results in such extensive isotope fractionation that little direct information can be obtained regarding sources. Recent measurements of natural  $^{14}\text{C-CH}_4$  show that the  $\text{CH}_4$  geochemistry in both basins is dominated (~64 to 98%) by inputs of fossil (radiocarbon-free)  $\text{CH}_4$  from seafloor seeps. We derive open-system kinetic isotope effect equations and use a one-dimensional (vertical) stable isotope box model that, along with isotope budgets developed using radiocarbon, permits a quantitative treatment of the stable isotope differences. We show that two main factors control the  $\text{CH}_4$  concentration and stable isotope differences: (1) the depth distributions of the input of  $\text{CH}_4$  from seafloor seeps and (2) anaerobic oxidation of  $\text{CH}_4$  under open-system steady state conditions in the Black Sea and open-system non-steady-state conditions in the Cariaco Basin.

**Citation:** Kessler, J. D., W. S. Reeburgh, and S. C. Tyler (2006), Controls on methane concentration and stable isotope ( $\delta^2\text{H-CH}_4$  and  $\delta^{13}\text{C-CH}_4$ ) distributions in the water columns of the Black Sea and Cariaco Basin, *Global Biogeochem. Cycles*, 20, GB4004, doi:10.1029/2005GB002571.

### 1. Introduction

[2] The Black Sea and Cariaco Basin are two large permanently anoxic basins that have been sites of numerous studies of methane ( $\text{CH}_4$ ) geochemistry [e.g., *Amouroux et al.*, 2002; *Atkinson and Richards*, 1967; *Ivanov et al.*, 2002; *Reeburgh*, 1976; *Reeburgh et al.*, 1991; *Scranton*, 1988; *Ward et al.*, 1987; *Wiesenburg*, 1975]. The source of  $\text{CH}_4$  to the water column in both of these basins was originally considered to be from sediment diagenesis [e.g., *Reeburgh*, 1976; *Reeburgh et al.*, 1991; *Scranton*, 1988]. A sink-based  $\text{CH}_4$  budget for the Black Sea was assembled from  $\text{CH}_4$  concentration ( $[\text{CH}_4]$ ) and oxidation rate measurements conducted in the water column and sediments at a central and shelf station in July 1988 [*Reeburgh et al.*, 1991]. This budget showed that the diffusive flux of  $\text{CH}_4$  from sediments was too small to balance the major  $\text{CH}_4$  sink from the water column, anaerobic oxidation of  $\text{CH}_4$  (AOM), suggesting an additional  $\text{CH}_4$  source. Subsequent reports of seeps,  $\text{CH}_4$  clathrate hydrates (clathrates), mud volcanoes, and

pockmarks [*Ginsburg et al.*, 1990; *Gulin et al.*, 2003; *Luth et al.*, 1999; *Michaelis et al.*, 2002; *Pape et al.*, 2003; *Vassilev and Dimitrov*, 2002], suggested that fossil (radiocarbon-free)  $\text{CH}_4$  may be the dominant source of  $\text{CH}_4$  to the Black Sea.

[3] The source of  $\text{CH}_4$  to the Cariaco Basin was first investigated with a steady state vertical advection-diffusion model [*Fanning and Pilson*, 1972; *Reeburgh*, 1976]. The steady state assumption used in these Cariaco Basin studies was later challenged and a time-dependent geochemical box model was developed to study  $\text{CH}_4$  geochemistry [*Scranton*, 1988; *Scranton et al.*, 1987]. Both steady state and non-steady-state investigations [*Reeburgh*, 1976; *Scranton*, 1988] concluded that AOM occurred, and that diffusion of  $\text{CH}_4$ , produced by diagenesis in the sediments ( $\text{CH}_{4[\text{D}]}$ ), provided the source to the water column. Recent natural radiocarbon measurements on Black Sea and Cariaco Basin  $\text{CH}_4$  ( $^{14}\text{C-CH}_4$ ) have shown that fossil  $\text{CH}_4$  emitted from seeps ( $\text{CH}_{4[\text{S}]}$ ), not  $\text{CH}_{4[\text{D}]}$ , is the dominant source to both water columns [*Kessler et al.*, 2006, 2005].

[4] Here we report  $[\text{CH}_4]$  and stable isotope ( $\delta^2\text{H-CH}_4$  and  $\delta^{13}\text{C-CH}_4$ ) measurements for the Black Sea and Cariaco Basin (Figures 1 and 2; Figure 3 for Cariaco Basin sediments; and Table 1 for Black Sea seeps). The similarities in  $\text{CH}_4$  sources, structure, and marine setting of both basins suggest that the  $\delta^2\text{H-CH}_4$  and  $\delta^{13}\text{C-CH}_4$  distributions in the water column might be similar, but the between-basin stable

<sup>1</sup>Department of Earth System Science, University of California Irvine, Irvine, California, USA.

<sup>2</sup>Now at Department of Geosciences, Princeton University, Princeton, New Jersey, USA.

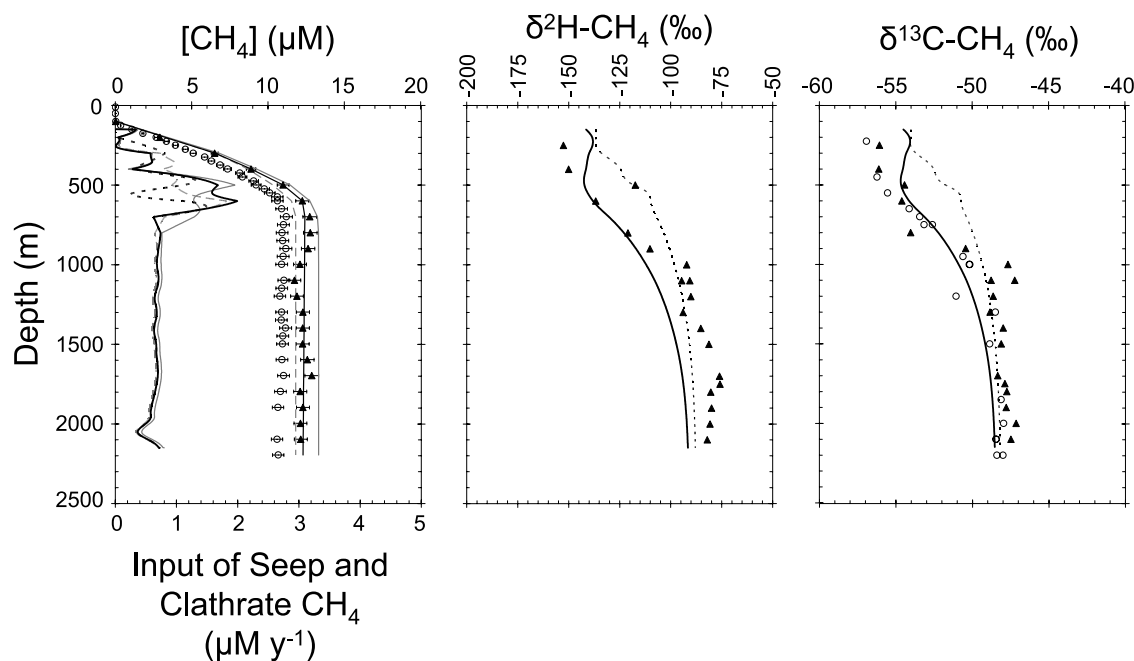


**Figure 1.** Measured Black Sea CH<sub>4</sub> stable isotope ( $\delta^2\text{H-CH}_4$  and  $\delta^{13}\text{C-CH}_4$ ) and  $[\text{CH}_4]$  ( $\mu\text{M}$ ) data collected in the water column in (triangles) May 2001 in the western Black Sea and (circles) July 1988 in the central Black Sea [Reeburgh *et al.*, 2006, 1991]. Precision of the (1)  $[\text{CH}_4]$  measurements is  $\pm 3\text{--}4\%$  based on replicate analyses of samples, (2)  $\delta^2\text{H-CH}_4$  measurements is  $2.4\text{‰}$  based on replicate analyses of standard samples, and (3)  $\delta^{13}\text{C-CH}_4$  measurements is  $0.2\text{‰}$  based on replicate analyses of standard samples. Error bars for the stable isotope measurements are less than the width of the data points. The black and gray bars (solid, dashed, and dotted) represent the model results in the Black Sea. Two different profiles for the eddy-diffusion coefficients were assigned: (solid black line and gray lines) 150–350 m:  $2\text{ cm}^2\text{ s}^{-1}$ , 350–650 m:  $3\text{ cm}^2\text{ s}^{-1}$ , 650–2150 m:  $4\text{ cm}^2\text{ s}^{-1}$ ; (dotted black line) 150–650 m:  $1.02\text{ cm}^2\text{ s}^{-1}$ , 650–2150 m:  $4.07\text{ cm}^2\text{ s}^{-1}$  [Scranton, 1988]. The model was initiated with uniform average values of the  $[\text{CH}_4]$  profile below 700 m depth (black lines) and with uniform upper and lower bounds of the  $[\text{CH}_4]$  profile (gray lines); the stable isotope models are insensitive to these changes in  $[\text{CH}_4]$ .

isotope differences are large. The CH<sub>4</sub> stable isotope results generally differ by ca.  $80\text{‰}$  for  $\delta^2\text{H-CH}_4$  and  $10\text{‰}$  for  $\delta^{13}\text{C-CH}_4$ , and the shapes of the distributions are mirror-images of one another (Figures 1 and 2). How can the Black Sea and Cariaco Basin have such strong first-order similarities, yet have such different  $[\text{CH}_4]$  and CH<sub>4</sub> stable isotope distributions? We compare the bathymetry, geological history and setting, controls on stratification, and circulation in both basins. We also consider previously measured concentrations, oxidation rates, turnover times, and radiocarbon ( $^{14}\text{C-CH}_4$ ) contents of CH<sub>4</sub> to study the geochemistry of CH<sub>4[S]</sub> in these two large anoxic basins. We derive an open-system stable isotope equation that can be applied to steady state and non-steady-state environments to determine the fractionation factor ( $\alpha$ ) for AOM that occurs in the water column, stable isotope signature of the CH<sub>4</sub> at the point of release to the water column, or the fraction of the flux of CH<sub>4</sub> to the water column that is oxidized. Finally, we develop one-dimensional (vertical) box models which indicate that the depth distribution of seep inputs to the water column and AOM are the main controls on these stable isotope distributions.

[5] Discoveries of carbonate structures, isotopically light carbonate cements, and seeping CH<sub>4</sub> around coastal-ocean

faults indicate that geological CH<sub>4</sub> may be a significant global CH<sub>4</sub> source in oceanic and global CH<sub>4</sub> and carbon cycles [Bernard *et al.*, 1976; Clark *et al.*, 2000; Gulin *et al.*, 2003; Judd, 2004; Kelley *et al.*, 2005; Leifer *et al.*, 2004; Michaelis *et al.*, 2002; Sansone *et al.*, 2001; Sassen *et al.*, 2001]. Studying the biogeochemistry of geological CH<sub>4</sub> is complicated in the coastal ocean by advection, mixing, and dilution [Sansone *et al.*, 2001; Valentine *et al.*, 2001]. However, the restricted deep water circulation of semi-enclosed basins allows CH<sub>4</sub> accumulation without ocean-scale dispersion and permits determination of fluxes of CH<sub>4</sub> to the water column averaged over large spatial scales [Kessler *et al.*, 2006, 2005]. The Cariaco Basin, and especially the Black Sea, are globally important CH<sub>4</sub> reservoirs, and the fossil CH<sub>4</sub> geochemistry in both basins may provide analogs to global fossil CH<sub>4</sub> geochemistry in the coastal ocean.

## 2. Experimental

[6] Water samples were collected from 26 May to 3 June 2001, on board the R/V *Knorr* within a 4.24 km radius of a station in the western section of the Black Sea ( $42^\circ 30.21'\text{N}$ ,  $30^\circ 45.21'\text{E}$ , 2100 m; Figure 4). Black Sea seep gas was

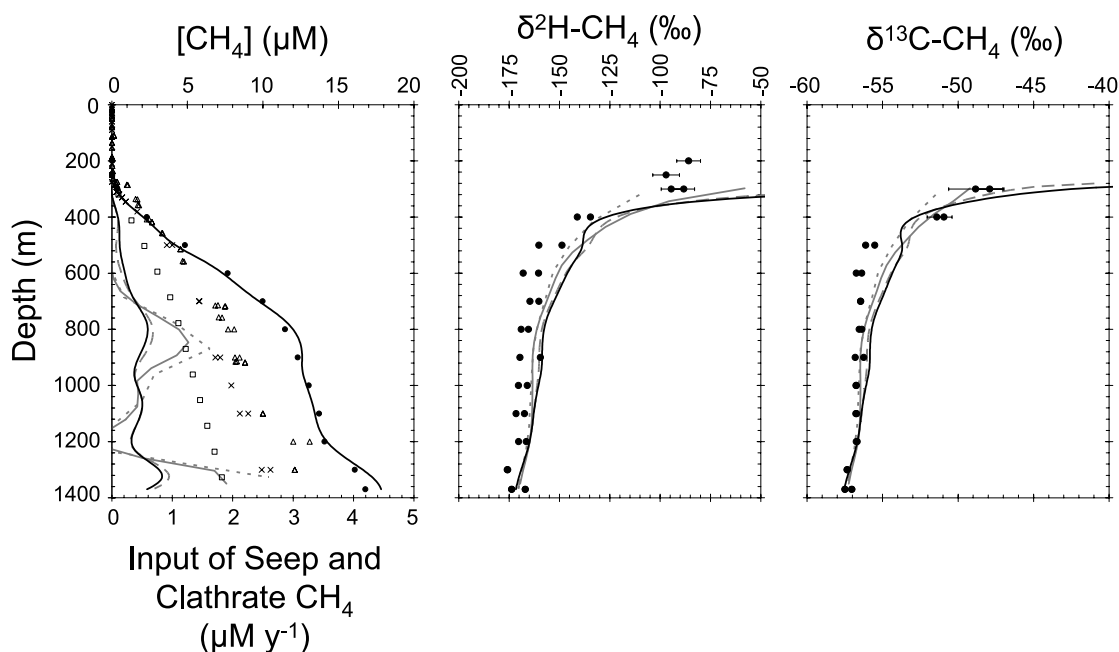


**Figure 2.** Measured Cariaco Basin CH<sub>4</sub> stable isotope ( $\delta^2\text{H-CH}_4$  and  $\delta^{13}\text{C-CH}_4$ ) and  $[\text{CH}_4]$  ( $\mu\text{M}$ ) data collected in the water column in (circles) January 2004 in the eastern basin, (triangles) February to March 1986 in the western basin [Ward *et al.*, 1987], (crosses) November 1982 [Scranton, 1988] in the western basin, and (squares) February 1974 in the eastern basin [Reeburgh, 1976; Wiesenburg, 1975]. The precisions are the same as in Figure 1. The black and gray lines (solid, dashed, and dotted) represent the model results in the Cariaco Basin; (gray dotted line)  $\Delta z = 92$  m; (solid gray line)  $\Delta z = 46$  m; (gray dashed line)  $\Delta z = 11.5$  m; (solid black line)  $\Delta z = 5.75$  m.

collected from 10–26 September 2004, on board the F/S *Poseidon* with the submersible *JAGO* (Figure 4). Five independent seeps located within a 0.56 km radius around 44°46.48'N, 31°59.42'E (average depth of 222 m) were sampled (Table 1). Water and sediment samples were collected in the Cariaco Basin from 21–24 January 2004, on board the B/O *Hermano Gines*. The station was located in the deepest portion of the eastern basin (10.5°N, 64.66°W, 1370 m) at the time-series station used by the CARbon Retention In A Colored Ocean (CARIACO) program [Astor *et al.*, 2003; Scranton *et al.*, 2001] (Figure 5).

[7] Methane concentrations were measured with a headspace equilibration technique. Samples were prepared for

seawater  $[\text{CH}_4]$  analyses by filling serum vials directly from Niskin bottles. The seawater vials were sealed and an ultrahigh-purity helium headspace was introduced by displacing an equal volume of water. For the Black Sea, 120 cc serum vials were used with a 10 cc helium headspace, while for the Cariaco Basin, 160 cc serum vials were used with a 13 cc helium headspace. Sediment samples for  $[\text{CH}_4]$  analyses were prepared by making a slurry of 3 cc of sediment (syringe subcores) and 6 cc of helium-purged water in sealed 37.5 cc serum vials. After the samples were allowed to equilibrate for at least 12 hours,  $[\text{CH}_4]$  analyses were performed by analyzing three 3 cc aliquots of the headspace with gas chromatography (GC) and flame ioni-

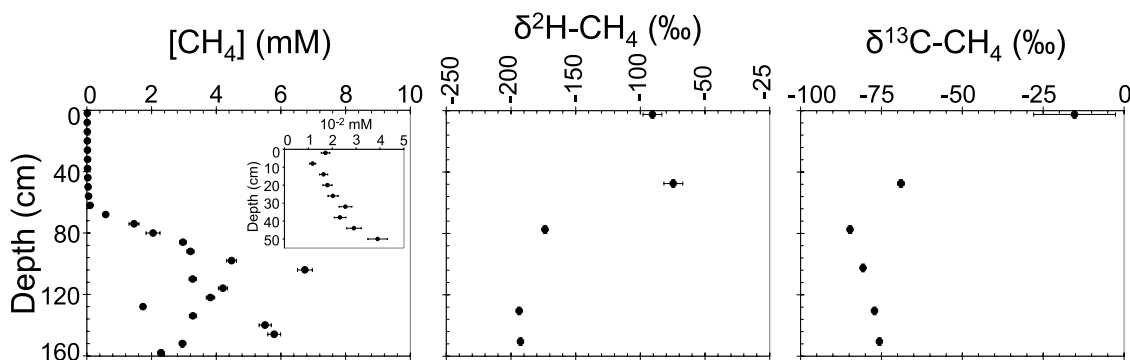


**Figure 3.** Cariaco Basin CH<sub>4</sub> stable isotope ( $\delta^2\text{H-CH}_4$  and  $\delta^{13}\text{C-CH}_4$ ) and  $[\text{CH}_4]$  (mM) data collected in the sediment in January 2004 in the eastern basin. The precisions are the same as in Figure 1. The inset shows  $[\text{CH}_4]$  from the top 55 cm replotted on an expanded concentration scale.

**Table 1.** Black Sea CH<sub>4</sub>[S] Isotope Data

Ship Station	Latitude, °N	Longitude, °E	Water Depth ± 4.3 m	δ <sup>13</sup> C-CH <sub>4</sub> ± 0.2‰	δ <sup>2</sup> H-CH <sub>4</sub> ± 2.4‰	<sup>14</sup> C-CH <sub>4</sub> ± 0.04 pMC
705	44°46.5′	31°59.5′	230	-67.0	-216.9	5.50
708	44°46.5′	31°59.7′	231	-67.6	-251.8	5.05
711	44°46.49′	31°59.55′	222	-67.6	-252.8	5.05
729	44°46.5′	31°59.5′	223	-67.5	-232.5	5.08
752	44°46.4′	31°58.86′	203	-67.8	-244.3	4.44

zation detection (FID) (GC-Mini 2; Shimadzu Corp.; carrier gas (N<sub>2</sub>) flow rate = 33 mL/min, column temp = 70°C, 1.5 m column packed with molecular sieve 5A 60/80 mesh). The Black Sea [CH<sub>4</sub>] profile was measured at sea. The Cariaco Basin [CH<sub>4</sub>] analyses were performed in our UCI laboratory, so all vials were poisoned with a saturated mercuric chloride solution and sealed with blue butyl rubber stoppers and crimp caps. The results have been corrected for the amount of CH<sub>4</sub> still dissolved in solution [Yamamoto *et al.*, 1976].

[8] A previously published procedure was used to collect and prepare CH<sub>4</sub> dissolved in water or sediment for isotopic analyses [Kessler and Reeburgh, 2005]. The CH<sub>4</sub> collection,

extraction, and analysis procedures are quantitative, there is no isotope fractionation, and the backgrounds are small (0.52<sub>8</sub> ± 0.39 μmoles of CH<sub>4</sub>) relative to the average sample size (220 μmoles). (To test the accuracy of the concentration profile measured in the Cariaco Basin by GC-FID in 2004, we calculated the [CH<sub>4</sub>] from the quantity of CH<sub>4</sub> collected for isotopic analyses. Both methods agreed within 3% on average below 300 m depth.)

### 3. Results

[9] Although the general shapes of both δ<sup>2</sup>H-CH<sub>4</sub> and δ<sup>13</sup>C-CH<sub>4</sub> profiles in the water column are similar in their

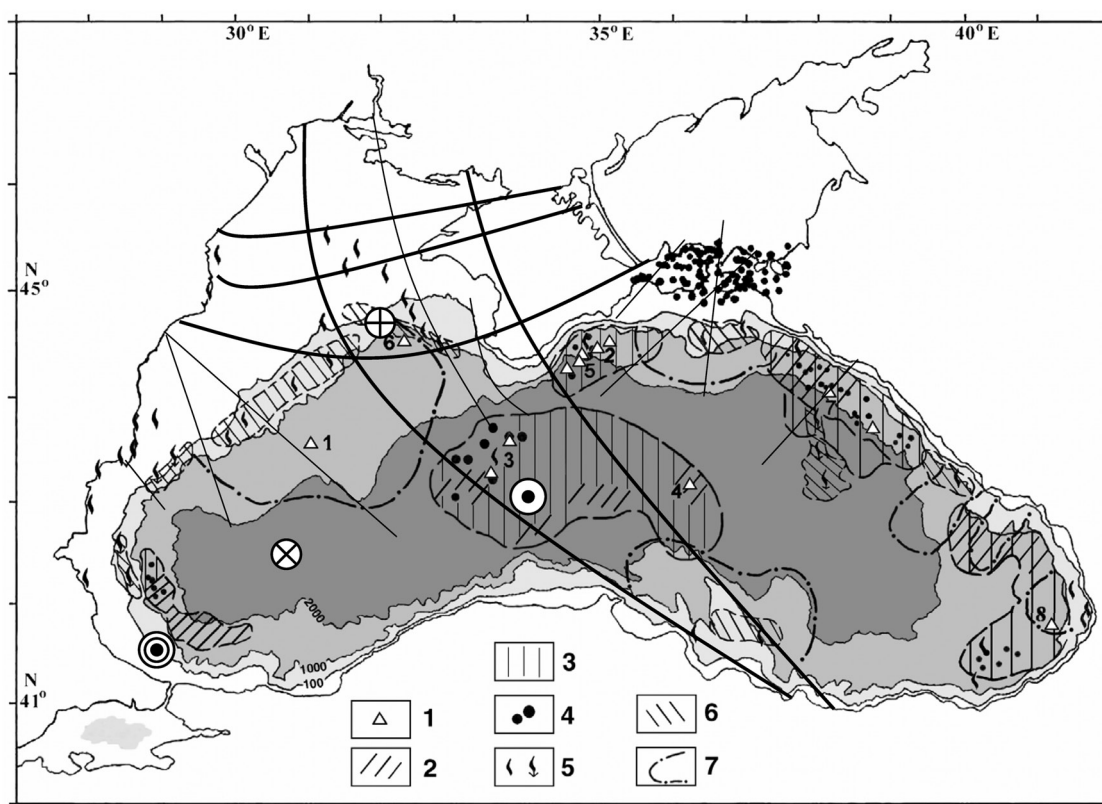


**Figure 4.** Black Sea sampling locations and deep faults: circle with dot, July 1988 sample site ([CH<sub>4</sub>], oxidation rates, and stable isotopes) [Reeburgh *et al.*, 2006, 1991]; double circle with dot, July 1988 shelf sample site ([CH<sub>4</sub>] in sediment); circle with cross, May 2001 sample site ([CH<sub>4</sub>] and isotopes in the water column); and circle with plus, September 2004 sample site (seep gas collection). The map is from Vassilev and Dimitrov [2002] with the following symbols: (1) Clathrate sampling (see Table 1 of Vassilev and Dimitrov [2002] for numbering); (2) areas with seismic indications of clathrates; (3) areas of high clathrates prospect; (4) mud volcanoes; (5) areas of intensive fluid discharging; (6) gas seepage and seabed pockmarks; and (7) mine submarine fans. The solid lines are deep faults interpolated after Kutas *et al.* [2004].

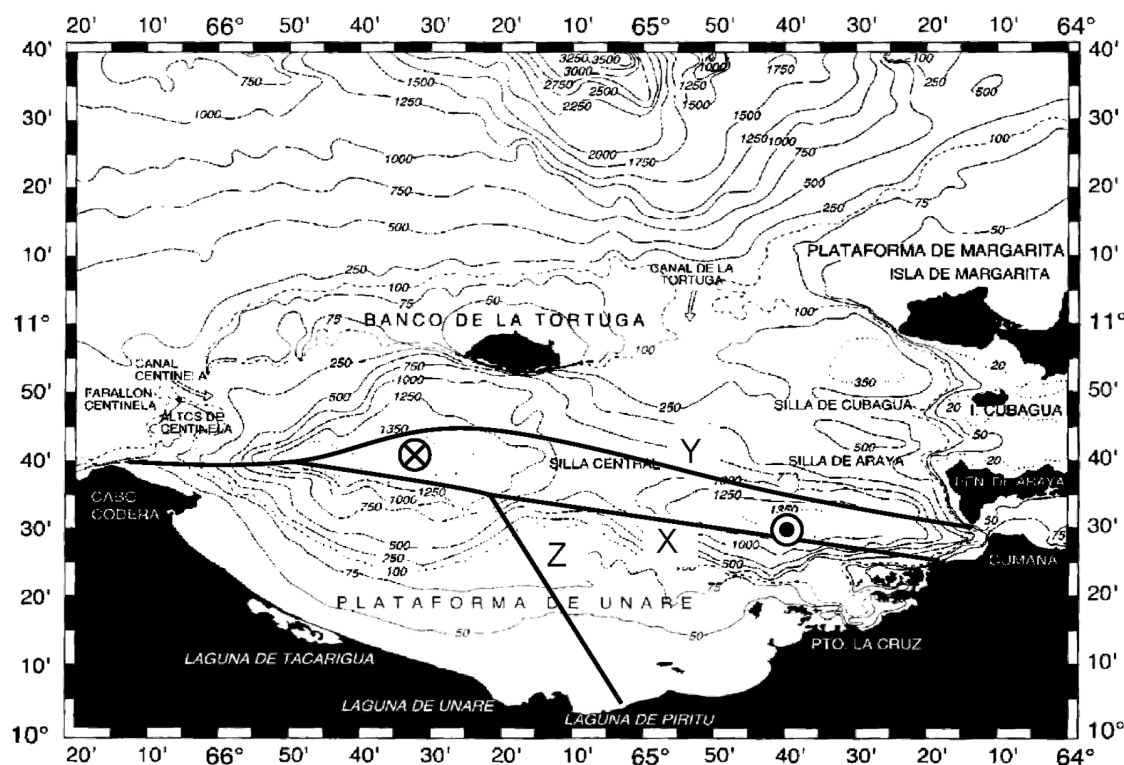


**Figure 5.** Cariaco Basin sampling locations and faults. The solid lines are faults interpolated after *Audemard et al.* [2005]. (X) El Pilar Fault; (Y) San Sebastián Fault; (Z) San Mateo Fault; circle with dot, eastern basin sampling site; and circle with cross, western basin sample site. The map is from *Scranton et al.* [2001].

respective basins, large differences are evident between the [CH<sub>4</sub>] and stable isotopes in the Black Sea and Cariaco Basin (Figures 1 and 2). The isotopically lightest CH<sub>4</sub> in the Black Sea is in the near surface waters (250 m depth;  $\delta^2\text{H} = -152.6 \pm 2.4\text{‰}$ ;  $\delta^{13}\text{C} = -56.1 \pm 0.2\text{‰}$ ) and becomes heavier almost linearly until a depth of 1000 m. Below 1000 m, the stable isotope signatures of CH<sub>4</sub> remain nearly uniform at  $-84.8 \pm 6.7\text{‰}$  and  $-48.0 \pm 0.6\text{‰}$  for  $\delta^2\text{H}$  and  $\delta^{13}\text{C}$ , respectively. Methane emitted from the sampled Black Sea seeps has a nearly uniform stable isotope signature ( $\delta^2\text{H} = -240 \pm 15\text{‰}$ ;  $\delta^{13}\text{C} = -67.5 \pm 0.3\text{‰}$ ; Table 1).

[10] The general shapes of Cariaco Basin  $\delta^2\text{H}\text{-CH}_4$  and  $\delta^{13}\text{C}\text{-CH}_4$  profiles in the water column are mirror-images of the Black Sea profiles (Figures 1 and 2). The isotopically heaviest CH<sub>4</sub> is in the upper water column (200–250 m depth;  $\delta^2\text{H} = -85.9 \pm 2.4\text{‰}$ ;  $\delta^{13}\text{C} = -9.8 \pm 0.2\text{‰}$  (not shown in Figure 2)) and becomes isotopically lighter until a depth of 600 m. Below 600 m, the isotopes of CH<sub>4</sub> are nearly uniform at  $-167.8 \pm 4.8\text{‰}$  and  $-56.7 \pm 0.5\text{‰}$  for  $\delta^2\text{H}$  and  $\delta^{13}\text{C}$ , respectively, which are 83‰ and 9‰ lighter than was measured in the Black Sea.

[11] We have no sediment stable isotope data for the Black Sea. The Cariaco Basin sediment profiles for  $\delta^2\text{H}\text{-CH}_4$  and  $\delta^{13}\text{C}\text{-CH}_4$  (Figure 3) are similar to observations from Skan Bay and Eckernförde Bay [*Alperin et al.*, 1988; *Martens et al.*, 1999]. The depth resolution presented here is

coarser than was measured in Skan Bay and Eckernförde Bay, so we may have missed additional features identified at these other sites. The isotopically heaviest CH<sub>4</sub> is in the near-surface sediments ( $\delta^2\text{H} = -115.9 \pm 2.4\text{‰}$ ;  $\delta^{13}\text{C} = -15.3 \pm 0.2\text{‰}$ ) most likely owing to isotopic fractionation caused by AOM. For  $\delta^2\text{H}\text{-CH}_4$ , the lightest value measured ( $-193.7 \pm 2.4\text{‰}$ ) occurs at 130.5 cm depth, while for  $\delta^{13}\text{C}\text{-CH}_4$ , the lightest value measured ( $-84.7 \pm 0.2\text{‰}$ ) occurs at 77.5 cm depth.

[12] The [CH<sub>4</sub>] measured in the water column of the western Black Sea in 2001 is on average 11.5% higher than that measured in the central basin in 1988 at depths below 600 m (Figure 1). This may be an indication of lateral heterogeneity or local sources. The Cariaco Basin [CH<sub>4</sub>] in the water column has steadily increased over the measurement history [*Scranton et al.*, 2001]. The bottom water [CH<sub>4</sub>] measured in January 2004 has more than doubled since February 1974 [*Kessler et al.*, 2005; *Reeburgh*, 1976; *Wiesenburg*, 1975] (Figure 2).

#### 4. Discussion

[13] To understand and quantify the large between-basin differences in stable isotope results, we review the geological settings, CH<sub>4</sub> budgets, <sup>14</sup>C-CH<sub>4</sub> distributions, and evolution of CH<sub>4</sub> in these systems (Table 2). This investi-

**Table 2.** Basin and Methane Characteristics for the Black Sea and Cariaco Basin

	Black Sea	Cariaco Basin
Width	41°–46°N (560 km)	10°21′–11°02′N (76 km)
Length	28°–42°E (1120 km)	64°12′–66°04′W (205 km)
Area, km <sup>2</sup>	423,000 <sup>a,b,c</sup>	8220 <sup>d,e</sup>
Volume, km <sup>3</sup>	534,000 <sup>a,b,c</sup>	730 for depths > 275 m <sup>d,e</sup>
Max depth, m	2200 <sup>a,b</sup>	E. Basin, 1370; W. Basin, 1400 <sup>d</sup>
Sill depth, m	32–34 <sup>f</sup>	E. Sill, 135; W. Sill 146 <sup>d,g</sup>
Water properties (T, S, $\sigma_\theta$ )		
Surface	25, 17.9, 10	23.4, 36.8, 25.19
Bottom	8.9, 22.3, 17.2	16.7, 36.18, 26.44
Depth of oxic/anoxic interface, m	100–150 m <sup>h</sup>	250–300 <sup>i</sup>
Onset of anoxia, years Before Present	7300–7540 <sup>b,j</sup>	12600 <sup>k</sup>
Freshwater inputs, km <sup>3</sup> yr <sup>-1</sup>		
Danube	198	
Dnepr	52	
Don	28	
Georgian coast	41	
Turkish coast	25	
Methane concentration, $\mu\text{M}$	basin center below 600 m: 10.9 <sup>h</sup> western basin below 600 m: 12.4 <sup>m</sup>	1974: Increasing to 7 <sup>l</sup> 1998: Increasing to 12.5 <sup>i</sup> 2004: Increasing to 16.8 <sup>n</sup> modeled: 0.0011–0.0153 <sup>p</sup> 0.15–0.3 <sup>e</sup> measured: year 1987: 0.0129–0.160 <sup>q</sup> year 2004: 0.04–0.19 <sup>q,m</sup>
Methane consumption rate, $\mu\text{M yr}^{-1}$	modeled: 0.015 <sup>o</sup>  measured: Surface 100 m: $0.36 \times 10^{-3}$ h Below 100 m: 0.6 <sup>h</sup>	modeled: 30–70 <sup>e</sup> measured: year 2004: 50–60 <sup>q</sup> 0.14–0.17 <sup>n</sup>
Methane Residence Time, years (year 2004)	modeled: 73 <sup>o</sup> measured: 3.6–18 <sup>h</sup>	
Inputs of CH <sub>4</sub> from seeps, mol m <sup>-2</sup> yr <sup>-1</sup>	0.53–0.84 <sup>m</sup>	

<sup>a</sup>Ross et al. [1974].<sup>b</sup>Deuser [1974].<sup>c</sup>Isakov [1953].<sup>d</sup>Maloney [1966].<sup>e</sup>Scranton [1988].<sup>f</sup>Latif et al. [1991].<sup>g</sup>Richards and Vaccaro [1956].<sup>h</sup>Reeburgh et al. [1991].<sup>i</sup>Scranton et al. [2001].<sup>j</sup>Jones and Gagnon [1994].<sup>k</sup>Peterson et al. [2000].<sup>l</sup>Wiesenburg [1975].<sup>m</sup>Kessler et al. [2006].<sup>n</sup>Kessler et al. [2005].<sup>o</sup>Scranton [1977].<sup>p</sup>Reeburgh [1976].<sup>q</sup>Ward et al. [1987].

gation leads to the derivation of two open-system stable isotope equations and a one-dimensional (vertical) geochemical box model of stable isotopes of CH<sub>4</sub>.

#### 4.1. Geological Setting

[14] The Black Sea, the world's largest anoxic basin (area =  $4.23 \times 10^5$  km<sup>2</sup>, max depth = 2200 m; Table 2), was formed as an extensional back-arc basin from the Late Cretaceous to the Eocene, and comprises the West and East Black Sea basins. Current geophysical data suggests that the Black Sea is closing under north-south compressional stress [Alptekin et al., 1986; Robinson et al., 1996; Zonenshain and Pichon, 1986]. During the Pleistocene and early Holocene, the Black Sea was an oxygenated fresh- or brackish-water body. The rise of global sea level 9000–9800 years before present (BP) caused an inflow of saline Mediterranean waters through the Bosphorus, which accumulated in the bottom of the basin. River runoff capped the saline bottom waters and led to a strong salinity stratification, impeding vertical mixing. Owing to this stratification, the

flux of oxygen to the deep basin was restricted to what was transported in by the Mediterranean water. The organic carbon transported to the deep basin far exceeded the input of dissolved oxygen, which led to anoxic conditions being established in the deep basin ca. 7300–7540 years BP [Deuser, 1974; Jones and Gagnon, 1994] (Table 2).

[15] In contrast, the area of the Cariaco Basin ( $8.22 \times 10^3$  km<sup>2</sup>) is significantly smaller than the Black Sea, and contains water whose salinity is close to adjacent open ocean values (Table 2). The continental transform associated with the El Pilar fault system in the Venezuelan borderland is most likely responsible for the formation of the Cariaco Basin; however, the exact tectonic mechanism for this basin's formation is currently unknown. During the Last Glacial Maximum (LGM), lowered sea level caused the Cariaco Basin to be nearly isolated from the Caribbean. The only connection with the open ocean would have been on the western end of the Cariaco Basin at a depth of <30 m. Although the Cariaco Basin was more isolated from the open ocean during the LGM than today, oxic conditions

persisted. This most likely occurred because the upwelling waters were nutrient limited which decreased the surface productivity and transport of organic carbon to the deep basin [Peterson *et al.*, 2000]. Increasing sea level at the end of the LGM allowed for more nutrient rich waters to be upwelled, increasing surface productivity and transport of organic matter to the deep basin. This organic matter flux overwhelmed the oxygen flux to the deep basin establishing the most recent anoxic conditions ca. 12600 year BP [Peterson *et al.*, 2000].

#### 4.2. CH<sub>4</sub> Budgets and Radiocarbon Analyses

[16] The dominant source of CH<sub>4</sub> into both basins has been regarded for the past 30 years as diagenetically-produced, diffusing from sediments. Reeburgh *et al.* [1991] conducted CH<sub>4</sub> concentration and oxidation rate measurements in the central Black Sea, determining that AOM was the dominant sink of CH<sub>4</sub> from the water column (70-fold larger than the next largest sink, evasion at the air:sea interface). The central station was chosen to represent a basin-wide integration of processes affecting the Black Sea CH<sub>4</sub> budget (Figure 4). The Black Sea water column CH<sub>4</sub> distribution was assumed to be in steady state, so the total sink of CH<sub>4</sub> from the water column must be matched with a source of the same magnitude. However, measurements of [CH<sub>4</sub>] in the sediments in shelf and deep basin cores indicate that 86.7% or more of the flux of CH<sub>4</sub> to the water column is not accounted for by diffusion from sediments [Ivanov *et al.*, 2002; Jørgensen *et al.*, 2001; Reeburgh *et al.*, 1991]. Reeburgh *et al.* [1991, 2006] concluded that large-scale methanogenesis does not occur in the anoxic Black Sea water column so long as sulfate reduction is occurring [Hoehler *et al.*, 1994, 1998]. Measurements by Albert *et al.* [1995], show that sulfate reduction occurs in the Black Sea water column at nM day<sup>-1</sup> rates.

[17] The source of CH<sub>4</sub> to the Cariaco Basin was previously investigated with [CH<sub>4</sub>] and oxidation rate measurements [Ward *et al.*, 1987] as well as vertical advection-diffusion and time-dependent box models [Reeburgh, 1976; Scranton, 1988; Scranton *et al.*, 2001]. These studies determined that AOM is the largest sink of CH<sub>4</sub> from the water column in the Cariaco Basin and that the CH<sub>4</sub> geochemistry can be explained with only a source of CH<sub>4[D]</sub>. While recent studies have shown that turbidity flows, mid-depth (250–350 m) intrusions of oxygenated water, and deep basin intrusions of hypersaline shelf water influence other constituents in the Cariaco Basin water column [Astor *et al.*, 2003; Holmén and Rooth, 1990; Scranton *et al.*, 2001], they have been shown to have only minor effects on CH<sub>4</sub> [Kessler *et al.*, 2005; Scranton *et al.*, 2001].

[18] Recent <sup>14</sup>C-CH<sub>4</sub> measurements in the Black Sea and Cariaco Basin confirm that the dominant source of CH<sub>4</sub> to these water columns is from fossil CH<sub>4</sub> and not from CH<sub>4[D]</sub> [Kessler *et al.*, 2006, 2005]. The CH<sub>4</sub> emitted from 5 different seeps in the Black Sea contained small but measurable amounts of radiocarbon (5.02 ± 0.4 pMC; Table 1), contrary to measurements in other oceanic locations [Grabowski *et al.*, 2004; Kessler, 2005; Kessler *et al.*, 2005; Winckler *et al.*, 2002a, 2002b] which indicated that CH<sub>4[S]</sub> is radiocarbon-free. A possible explanation why Black Sea

CH<sub>4[S]</sub> is not radiocarbon-free is that fossil petrogenic CH<sub>4</sub>, generated from Late Eocene age source rock [Robinson *et al.*, 1996], acquires modern CH<sub>4</sub> during transit through recently deposited sediments.

[19] Studies of CH<sub>4</sub> dissolved in anoxic sediments indicate that CH<sub>4</sub> can have near-modern <sup>14</sup>C-CH<sub>4</sub> contents in shallow (<100 cm depth) sediments [Kessler, 2005; Kessler *et al.*, 2005] as well as decadal turnover times, as calculated from measured [CH<sub>4</sub>] and rates of AOM [Iversen and Jørgensen, 1985; Reeburgh, 1980; Reeburgh *et al.*, 1991]. Methane dissolved in the Black Sea water column has similar decadal turnover times to CH<sub>4[D]</sub> [Reeburgh *et al.*, 1991] (Table 2). The <sup>14</sup>C-CH<sub>4</sub> results indicate that the source of CH<sub>4</sub> to the Black Sea water column is a mixture of CH<sub>4[S]</sub> and CH<sub>4[D]</sub>, because (1) CH<sub>4</sub> produced in shallow sediments has near-modern radiocarbon-contents, (2) CH<sub>4[S]</sub> is nearly radiocarbon-free, and (3) this oceanic CH<sub>4</sub> has decadal turnover times. The concentration-weighted average of the <sup>14</sup>C-CH<sub>4</sub> results in the Black Sea water column (15.72 ± 6.75 percent Modern Carbon [pMC] [Stuiver and Polach, 1977]) was used to show that between 64 to 98% of the source flux is from fossil CH<sub>4</sub> [Kessler *et al.*, 2006]. Also, the <sup>14</sup>C-CH<sub>4</sub> and [CH<sub>4</sub>] results were used to estimate the basin-wide source flux of CH<sub>4[S]</sub> to the Black Sea water column (3.6 to 5.7 Tg yr<sup>-1</sup> or 0.53 to 0.84 mol m<sup>-2</sup> yr<sup>-1</sup>) [Kessler *et al.*, 2006].

[20] The Cariaco Basin water column radiocarbon results clearly indicate CH<sub>4[D]</sub> is not the source of CH<sub>4</sub> to the water column. The water column is dominated by fossil CH<sub>4</sub> inputs (<sup>14</sup>C-CH<sub>4</sub> = 2.5 ± 0.2 pMC) while CH<sub>4[D]</sub> contained significant radiocarbon contents (86.4 pMC at 45 cm depth) [Kessler *et al.*, 2005]. Since the rates of AOM and [CH<sub>4</sub>] in the Cariaco Basin are neither uniform nor in steady state, the CH<sub>4</sub> turnover time in year 2004 was calculated by dividing the total quantity of CH<sub>4</sub> in the basin by the total loss of CH<sub>4</sub> due to AOM; this analysis indicates that the turnover time of CH<sub>4</sub> in the water column is 50–60 years (Table 2). Since the Cariaco Basin is too warm (16.9°C) for clathrates to be stable [Dickens and Quinby-Hunt, 1994], the CH<sub>4</sub> dissolved in the water column is almost devoid of radiocarbon, the CH<sub>4[D]</sub> (CH<sub>4</sub> dissolved in near surface sediments) contains modern quantities of radiocarbon, and the CH<sub>4</sub> has decadal turnover times, then large inputs of fossil CH<sub>4[S]</sub> must be the source of CH<sub>4</sub> to the water column [Kessler *et al.*, 2005]. In order to quantify the fossil CH<sub>4</sub> input to the water column, Scranton's [1988] time-dependent Cariaco box model was modified to include a source term for CH<sub>4[S]</sub> [Kessler *et al.*, 2005]. This model was evaluated with and without middepth intrusions of oxygenated water showing that the source of CH<sub>4[S]</sub> to the Cariaco Basin likely ranges from 0.024–0.028 Tg yr<sup>-1</sup> (0.14–0.17 mole m<sup>-2</sup> yr<sup>-1</sup>). This model predicted that there are large inputs of CH<sub>4[S]</sub> below 700 m depth.

[21] Both basins are tectonically active, containing major faults [Alptekin *et al.*, 1986; Audemard *et al.*, 2005; Kutas *et al.*, 2004; Mendoza, 2000; Robinson *et al.*, 1996; Suárez and Nábelek, 1990], which may provide the pathway for geological CH<sub>4</sub> to be emitted. The Black Sea is cross-cut by seven deep interregional and regional fault systems which have been correlated with heat flow and gas release [Kutas

*et al.*, 2004] (Figure 4). The Cariaco Basin is bordered and possibly cross-cut by the San Mateo Fault, El Pilar Fault, and San Sebastián Fault [Audemard *et al.*, 2005; Mendoza, 2000; Suárez and Nábelek, 1990], however, the exact locations of these faults within the basin are unknown (Figure 5). Also, a turbidity flow, correlated with the 9 July 1997 earthquake, has been observed in the Cariaco Basin [Thunell *et al.*, 1999]. More recently, a modeling study suggests a 1967 earthquake might have initiated the release of fossil CH<sub>4</sub> into the Cariaco Basin [Kessler *et al.*, 2005].

### 4.3. Open-System Stable Isotope Equations

[22] Conventional stable isotope equations describing mixing and kinetic isotope effects are not applicable to the Black Sea and Cariaco Basin. Several studies indicate that seep inputs are heterogeneously distributed across both basins [e.g., Gulin *et al.*, 2003; Kessler *et al.*, 2006, 2005; Vassilev and Dimitrov, 2002]. Studies of stable isotope mixing (e.g., Keeling plots [Keeling, 1958, 1961; Pataki *et al.*, 2003]) are not applicable to these basins because they do not account for the large isotopic fractionation associated with AOM [Alperin *et al.*, 1988; Martens *et al.*, 1999] and the heterogeneous distribution of inputs. Also, conventional stable isotope equations considering kinetic isotope effects assume a “closed system” (i.e., a fixed amount of reactant is allowed to partially react) [Bigeleisen and Wolfsberg, 1958]. The Black Sea and Cariaco Basin are “open systems,” where geological CH<sub>4</sub> is continuously added to the water column from seeps, while CH<sub>4</sub> is being removed simultaneously by anaerobic oxidation.

[23] We derive open-system stable isotope equations that account for the continuous input of geological CH<sub>4</sub> to the water column and the isotopic fractionation associated with AOM. These equations can be used to determine the fractionation factor for AOM in the water column, the stable isotope signature of the CH<sub>4</sub> at the point of release to the water column, or the fraction of the input flux of CH<sub>4</sub> to the water column that is oxidized. This derivation assumes: (1) CH<sub>4</sub> is being added to the system at a constant rate with a constant isotope signature, (2) no CH<sub>4</sub> was in the system before the source was turned on, (3) CH<sub>4</sub> is well mixed in the system, and (4) the removal of CH<sub>4</sub>, principally by oxidation, is proportional to the amount of CH<sub>4</sub> in the system and is the only cause of isotope fractionation. These equations were derived in a similar manner to equations describing kinetic isotope effects in a “closed system” [Bigeleisen and Wolfsberg, 1958]. Consider the two reactions



Assuming the reaction is first order in  $A$  and  $A'$  (or pseudo-first order due to high concentrations of  $B, C, \dots$ ), it follows

$$\frac{dA}{dt} = r_1 - kAB^bC^c \dots \quad (1)$$

$$\frac{dA'}{dt} = r_2 - k'A'B^bC^c \dots \quad (2)$$

Here  $A$  is the CH<sub>4</sub> molecule containing the heavy isotope,  $A'$  is the CH<sub>4</sub> molecule containing the light isotope,  $r_1$  is the constant rate of addition of  $A$ ,  $r_2$  is the constant rate of addition of  $A'$ , and  $k$  and  $k'$  are the rate constants for the reactions.

[24] Integration of these rate laws leads to the following equations.

$$\ln\left(\frac{r_1 - kAB^bC^c}{r_1}\right) = -kB^bC^ct \quad (3)$$

$$\ln\left(\frac{r_2 - k'A'B^bC^c}{r_2}\right) = -k'B^bC^ct \quad (4)$$

[25] Dividing equation (3) by equation (4) and simplifying, leads to equation (5),

$$\ln\left[\frac{1}{R_s} \frac{r_1 - kAB^bC^c}{r_2 - k'A'B^bC^c}\right] = \left(\frac{k}{k'} - 1\right) \ln\left(1 - \frac{k'A'B^bC^c}{r_2}\right), \quad (5)$$

where  $R_s$  is the isotopic ratio of the source CH<sub>4</sub> =  $r_1/r_2$ . The following substitutions are used to simplify equation (5):  $Rt$  is the isotopic ratio of the CH<sub>4</sub> in the reservoir at time  $t = A/A'$ ,  $\alpha$  is the isotopic fractionation factor =  $k'/k$ , and  $f$  is ratio of CH<sub>4</sub> oxidation to CH<sub>4</sub> input rates. Since the natural abundances of <sup>2</sup>H and <sup>13</sup>C are about 0.016% and 1% of <sup>1</sup>H and <sup>12</sup>C, respectively, and since the kinetic isotope effect is too small to change the concentration of the heavy isotope significantly beyond the 1% level, then the rate of addition and loss of the heavy isotope is much less than that of the light isotope.

$$kAB^bC^c + k'A'B^bC^c \approx k'A'B^bC^c$$

$$r_1 + r_2 \approx r_2$$

These substitutions simplify  $f$ ,

$$f = \frac{kAB^bC^c + k'A'B^bC^c}{r_1 + r_2} \approx \frac{k'A'B^bC^c}{r_2}$$

and can be used to further simplify equation (5).

$$\ln\left[\frac{1}{R_s} \frac{r_1 - kAB^bC^c}{r_2 - r_2f}\right] = \left(\frac{1}{\alpha} - 1\right) \ln(1 - f).$$

This equation further simplifies to

$$\ln\left[\frac{R_s - \frac{1}{\alpha}Rtf}{R_s(1-f)}\right] = \ln(1-f)^{1/\alpha-1}$$

Taking the exponential of both sides and solving for  $R_s$  leads to equation (6)

$$R_s = \frac{fRt}{\alpha - \alpha(1-f)^{1/\alpha}}, \quad (6)$$

which we convert to delta notation, yielding equation (7).

$$\delta S = \frac{f(\delta W + 1000)}{\alpha - \alpha(1-f)^{1/\alpha}} - 1000. \quad (7)$$

Here  $\delta S = (Rs/Rstd - 1) \times 1000$ ,  $\delta W = (Rt/Rstd - 1) \times 1000$ , and  $Rstd$  = the isotopic ratio of the standard.

[26] In the steady state case where  $f = 1$ , equation (7) simplifies to

$$\delta S = \frac{1}{\alpha}(\delta W + 1000) - 1000. \quad (8)$$

[27] Equation (8) can also be derived by equating equations (1) and (2) with 0, dividing the two equations, and simplifying. Step-by-step derivations of equations (7) and (8) are given by *Kessler* [2005].

#### 4.3.1. Black Sea: Testing the Steady State Assumption and Determining the Fractionation Factor for AOM in the Water Column

[28] The  $\delta^{13}\text{C-CH}_4$  results suggest that the CH<sub>4</sub> dissolved in the waters of the Black Sea is isotopically homogeneous (laterally) and in steady state. The  $\delta^{13}\text{C-CH}_4$  results collected in 2001 in the western Black Sea are similar to those collected in 1988 at the central station [*Reeburgh et al.*, 2006] (Figure 1). If a reservoir changes to an isotopically different source (e.g., a shift from a CH<sub>4[D]</sub> source to a CH<sub>4[S]</sub> source) or if the isotopic ratio of the source remains constant but the flux changes, then an isotopic shift will occur in the reservoir. The timescales for changes in the isotope ratio and the large-scale spatial isotopic gradients of a reservoir are often longer than they are for changes in total CH<sub>4</sub> [*Tans*, 1997]. Thus isotopic steady state is reached after concentration steady state. Since the  $\delta^{13}\text{C-CH}_4$  results show no spatial or temporal variability, they suggest that the Black Sea is in steady state with respect to CH<sub>4</sub>. A similar conclusion can be reached when incorporating these  $\delta^{13}\text{C-CH}_4$  measurements into equation (7). At depths  $\geq 1000$  m,  $\delta^{13}\text{C-CH}_4 = -48.9 \pm 1.1$  in year 1988 and  $-48.0 \pm 0.6$  in year 2001 (Figure 1). In addition, the previously determined fractionation factors for aerobic and anaerobic oxidation of CH<sub>4</sub> range from approximately 1.01 to 1.02 [*Reeburgh*, 2003]. Since we also measured  $\delta^{13}\text{C-CH}_{4[S]}$ , we use equation (7) to calculate the fraction of the CH<sub>4</sub> input that is oxidized ( $f$ ). This analysis indicates that  $f = 1$  when  $\alpha = 1.021 \pm 0.001$ , indicating that the CH<sub>4</sub> dissolved in the Black Sea water column is in steady state. It should be noted that the previously determined fraction factors for AOM were determined in a sediment environment, while the AOM we are studying occurs in the water column.

[29] If the Black Sea is rigorously determined to be in steady state, the stable isotope results of CH<sub>4[S]</sub> and CH<sub>4</sub> dissolved in the water column below 1000 m depth (where the basin is well mixed vertically and mixing along an isotopic gradient does not occur) can now be used with Equation 8 to calculate the  $\alpha$  for AOM that occurs in the water column. For  $\delta^2\text{H-CH}_4$  and  $\delta^{13}\text{C-CH}_4$ ,  $\alpha$  equals  $1.20_4 \pm 0.02_5$  and  $1.021 \pm 0.001$ , respectively. These fractionation factors for AOM in the water column are larger than was previously determined in sedimentary environments [*Alperin et al.*, 1988; *Martens et al.*, 1999]. If the horizontal transport of CH<sub>4</sub> from the seep site to the western basin sampling site is not fast relative to AOM, horizontal gradients in the stable isotopes will occur. This effect would lower our values for  $\alpha$ , making the values we

present here upper bounds on the true values. However, such horizontal gradients are not observed between our western and central basin sites (Figure 1).

#### 4.3.2. Cariaco Basin: Determining the Stable Isotope Signature of CH<sub>4[S]</sub>

[30] The open-system non-steady-state stable isotope equation (equation (7)) can be used to predict the stable isotope signature of this CH<sub>4[S]</sub> at the point of release into the water column since we know the stable isotope signature of CH<sub>4</sub> dissolved in the water column ( $\delta W$ ), the ratio of CH<sub>4</sub> input to oxidation rates ( $f$ ), and  $\alpha$  for AOM. (Below 600 m, the water column stable isotope signatures are relatively uniform at  $-167.8 \pm 4.8\%$  and  $-56.7 \pm 0.5\%$  for  $\delta^2\text{H-CH}_4$  and  $\delta^{13}\text{C-CH}_4$ , respectively (Figure 2). Modifications of *Scranton's* [1988] time-dependent model [*Kessler et al.*, 2005], estimate that  $0.024\text{--}0.028$  Tg CH<sub>4[S]</sub> yr<sup>-1</sup> are added to the water column, while the specific oxidation rates [*Ward et al.*, 1987] indicate that  $0.01$  Tg CH<sub>4[S]</sub> yr<sup>-1</sup> are being oxidized in 2004.) Thus the stable isotope signatures of the source CH<sub>4</sub> at the point of release into the water column are calculated to be  $-196.6 \pm 5.5$  to  $-202.3 \pm 5.8\%$  and  $-60.70 \pm 0.53$  to  $-61.50 \pm 0.55\%$  for  $\delta^2\text{H-CH}_4$  and  $\delta^{13}\text{C-CH}_4$ , respectively.

#### 4.4. Vertical Time-Dependent Box Model for Stable Isotopes

[31] *Scranton et al.* [1987] developed a time-dependent vertical box model which was later used to describe the Cariaco Basin CH<sub>4</sub> geochemistry in the water column [*Scranton*, 1988]. Following the radiocarbon confirmation that seeps are a dominate source of CH<sub>4</sub> to both basins, *Scranton's* model was modified to calculate possible depth distributions of inputs of CH<sub>4[S]</sub> and basin-wide fluxes of CH<sub>4[S]</sub> to the water column for both the Cariaco Basin and the Black Sea [*Kessler et al.*, 2006, 2005]. Conceptual diagrams of the original model are given by *Scranton et al.* [1987] and *Scranton* [1988].

[32] Here we further modified the basic skeleton of this model to study the depth distributions of the stable isotopes in both basins.

$$\begin{aligned} \frac{dn_i}{dt} = & (F_{Sedi} - F_{Ai})(A_i - A_{i+1}) + F_{Si}V_i - k_iC_iV_i \\ & + K_i \frac{(C_{i-1} - C_i)}{\Delta z} A_i + K_{i+1} \frac{(C_{i+1} - C_i)}{\Delta z} A_{i+1}. \end{aligned} \quad (9)$$

For box  $i$ ,  $dn_i/dt$  is the rate of change of the number of moles of CH<sub>4</sub>,  $F_{Sedi}$  is the input of CH<sub>4[D]</sub> (moles per area per time),  $F_{Ai}$  is the oxidation of water column CH<sub>4</sub> by abyssal sediments (moles per area per time),  $F_{Si}$  is the input of CH<sub>4[S]</sub> (moles per volume per time),  $k_i$  is the specific rate of AOM (per time),  $V_i$  is the volume,  $A_i$  and  $A_{i+1}$  are the basin areas at the top and bottom of the box,  $K_i$  and  $K_{i+1}$  are the eddy diffusion coefficients at the top and bottom of the box (area per time),  $C_i$  is the [CH<sub>4</sub>] in the box, and  $C_{i-1}$  and  $C_{i+1}$  are the [CH<sub>4</sub>] in boxes  $i - 1$  and  $i + 1$ . The area of sediment intersecting each box is calculated by subtracting  $A_{i+1}$  from  $A_i$ ; since the boxes are three-dimensional and the walls are sloped, this leads to a maximum error in the sediment area of  $<5\%$  [*Scranton et al.*, 1987].

[33] Equation (9) was used to solve for  $F_S$ , a vertical profile of the input of CH<sub>4[S]</sub> [Kessler *et al.*, 2006, 2005].  $F_S$  was then used to predict profiles of  $\delta^2\text{H-CH}_4$  and  $\delta^{13}\text{C-CH}_4$  in the water column of the Black Sea and Cariaco Basin using equations (10) and (11). The “L” and “H” subscripts denote the light and heavy isotopes.

$$\frac{dn_{Li}}{dt} = (F_{LSedi} - F_{LAI})(A_i - A_{i+1}) + F_{LSi}V_i - k_{Li}C_{Li}V_i + K_i \frac{(C_{Li-1} - C_{Li})}{\Delta z} A_i + K_{i+1} \frac{(C_{Li+1} - C_{Li})}{\Delta z} A_{i+1} \quad (10)$$

$$\frac{dn_{Hi}}{dt} = (F_{HSedi} - F_{HAI})(A_i - A_{i+1}) + F_{HSi}V_i - k_{Hi}C_{Hi}V_i + K_i \frac{(C_{Hi-1} - C_{Hi})}{\Delta z} A_i + K_{i+1} \frac{(C_{Hi+1} - C_{Hi})}{\Delta z} A_{i+1}. \quad (11)$$

Here

$$\begin{aligned} MIR_i &= (F_{Sedi} - F_{Ai})(A_i - A_{i+1}) + F_{Si}V \\ MIR_{Li} &= (F_{LSedi} - F_{LAI})(A_i - A_{i+1}) + F_{LSi}V \\ MIR_{Li} &= \frac{MIR_i}{1 + \left(\frac{\partial MI}{1000} + 1\right)R_{STD}} \\ k_{Li} &= \alpha k \frac{C_L + C_H}{\alpha C_L + C_H} \\ MIR_{Hi} &= (F_{HSedi} - F_{HAI})(A_i - A_{i+1}) + F_{HSi}V \\ MIR_{Hi} &= \frac{MIR_i \left(\frac{\partial MI}{1000} + 1\right)R_{STD}}{1 + \left(\frac{\partial MI}{1000} + 1\right)R_{STD}} \\ k_{Hi} &= k \frac{C_L + C_H}{\alpha C_L + C_H} \end{aligned}$$

Also,  $\delta_{MI}$  is the isotopic signature of CH<sub>4</sub> input into each box. For both basins, we assume that  $\delta_{MI}$  is uniform over the entire basin and is the same for both  $F_{Sedi}$  and  $F_{Si}$ . Also, we assume that the rate of horizontal mixing is fast relative to AOM and that  $F_{Ai}$  only causes isotopic fraction of residual CH<sub>4</sub> in the sediment, not the water column. (Tables of the input parameters for these models are found in the auxiliary material<sup>1</sup>.)

#### 4.4.1. Black Sea

[34] For the Black Sea, box volume and areas were obtained from Ross *et al.* [1974] and Deuser [1974], specific rates of AOM were previously measured by Reeburgh *et al.* [1991] to be uniform at 0.06 yr<sup>-1</sup>, and box depths ( $\Delta z$ ) were set equal to 1.5625 m as decreasing the box depth further did not cause significant changes in the final results. The eddy diffusion coefficients previously reported by Scranton [1988] were used here and were varied to assess the models’ sensitivities to this parameter. We use piecewise cubic splines to interpolate between the measurements obtaining values for the input parameters at the depth of each box. (See Table S1 in auxiliary material for the Black Sea model input parameters.) Since it is in steady state, equation (9) was set equal to zero and the equation was solved for  $F_{Si}$ . The

measurements of [CH<sub>4</sub>] in the water column conducted in year 2001 were used to predict  $F_{Si}$  for each box (Figure 1).

[35] Equations (10) and (11) were used to predict profiles of  $\delta^2\text{H-CH}_4$  and  $\delta^{13}\text{C-CH}_4$  in the water column. For the Black Sea, we assume  $\delta_{MI}$  equals the mean of our seep gas measurements ( $-240\text{‰}$  for  $\delta^2\text{H}$  and  $-67.5\text{‰}$  for  $\delta^{13}\text{C}$ ; Table 1) and use Newton-Raphson’s Method to solve this system of non-linear equations for  $C_L$  and  $C_H$ . This steady state vertical stable isotope model also provides supporting evidence that the Black Sea is in steady state; equations (9)–(11) were evaluated in a steady state manner (i.e., they were set equal to zero and solved) and the modeled and measured isotope results showed close agreement.

[36] In order to test our assumptions that  $\delta_{MI}$  is uniform over the entire basin, is similar for both  $F_{Sedi}$  and  $F_{Si}$ , and mixes fast horizontally relative to AOM, we used equations (10) and (11) along with an interpolation to the measured water column profiles of  $\delta^2\text{H-CH}_4$  and  $\delta^{13}\text{C-CH}_4$  to model a profile of  $\delta_{MI}$ . (See Table S1 in auxiliary material for the interpolated profiles of  $\delta^2\text{H-CH}_4$  and  $\delta^{13}\text{C-CH}_4$ , which are input into this calculation.) This analysis produces a relatively uniform distribution of  $\delta_{MI}$  below 300 m depth ( $\delta^2\text{H-CH}_4 = -241.3 \pm 39.5\text{‰}$  and  $\delta^{13}\text{C-CH}_4 = -67.7 \pm 4.1\text{‰}$ ), similar to our measurements (Table 1) and our model assumptions.

[37] Model sensitivities to variations in the [CH<sub>4</sub>] profile in the water column, the eddy-diffusion coefficients ( $K$ ), and the isotopic fractionation factors were tested. In general, the models are most sensitive to these parameter changes above 800 m depth and the model used to predict a profile of  $F_S$  shows a higher sensitivity to these parameters than the stable isotope model. The stable isotope model is more sensitive to changes in  $K$  than [CH<sub>4</sub>]. Changing the average values of  $\alpha$  to the bounds of the standard deviations causes no changes for the  $\delta^{13}\text{C-CH}_4$  results; however, it does result in average changes of 9 to 17% for  $\delta^2\text{H-CH}_4$  (see Table S3 in the auxiliary material).

[38] The measured and modeled  $\delta^2\text{H-CH}_4$  and  $\delta^{13}\text{C-CH}_4$  results in the water column are most similar to the CH<sub>4[S]</sub> values in the upper water column (Figure 1 and Table 1). The spatial distribution of model predicted (Figure 1) [Kessler *et al.*, 2006] and experimentally identified Black Sea seeps shows that most seeps are located on the shelf above 1000 m depth (Figure 4), and add CH<sub>4</sub> directly to the upper water column [Gulin *et al.*, 2003; Lüdmann *et al.*, 2004; Luth *et al.*, 1999; Michaelis *et al.*, 2002; Vassilev and Dimitrov, 2002] as well as to the atmosphere [Dimitrov, 2002]. The short residence time of CH<sub>4</sub> in the upper water column results in less oxidation and greater similarity to the source CH<sub>4</sub>.

#### 4.4.2. Cariaco Basin

[39] For the Cariaco Basin, the box volumes, areas, and eddy diffusion coefficients were obtained from Scranton [1988] and specific rates of AOM were previously measured by Ward *et al.* [1987]. Scranton *et al.* [1987] originally defined the boxes to have a depth ( $\Delta z$ ) of 50 fathoms (92 m) and subsequent adaptations of this model [Holmén and Rooth, 1990; Kessler *et al.*, 2005; Scranton, 1988] followed this convention. When using this model to solve for a profile of  $F_S$ , we find that it is not until the “conventional” box depth is divided by at least a factor

<sup>1</sup>Auxiliary materials are available at <ftp://ftp.agu.org/apend/gb/2005gb002571>.

of 16 (so that  $\Delta z = 5.75$  m) that this model becomes insensitive to changes in the box depth (Figure 2). (We use piecewise cubic splines to interpolate between the measurements obtaining values for the input parameters at the depth of each box. See Table S2 in the auxiliary material for the Cariaco Basin model input parameters.)

[40] Since the Cariaco Basin is not in steady state, a time-dependent iteration was used to solve equation (9) for  $F_S$ . The Cariaco Basin model as initiated with no CH<sub>4</sub> corresponding to year 1967 [Kessler et al., 2005] and an initial guess at the profile of  $F_S$  was assigned. The model was run for 37 years (until year 2004 corresponding to when our samples were collected) at a time step of 0.0001 years. (Decreasing the time step further did not change the results significantly.)  $F_S$  was modified and the model was reevaluated until the modeled 2004 [CH<sub>4</sub>] profile showed close agreement with the measured 2004 [CH<sub>4</sub>] profile.

[41] The stable isotope equations (equations (10) and (11)), were similarly evaluated in a time-dependent fashion. For the Cariaco Basin, we assume  $\delta_{MI}$  equals the results obtained from the open-system non-steady-state stable isotope equation ( $\delta^2\text{H-CH}_4 = -199.4\text{‰}$  and  $\delta^{13}\text{C-CH}_4 = -61.1\text{‰}$ ).

[42] The model-predicted inputs of CH<sub>4[S]</sub> show large inputs in the deep basin and none on the shallow shelves, unlike the Black Sea (Figure 2). Once CH<sub>4</sub> is released to the deep basin, it can diffuse toward the shallow water. This CH<sub>4</sub> is partially oxidized as it diffuses upwards, leaving the CH<sub>4</sub> dissolved in the near surface waters most isotopically enriched in the heavy isotopes. In the deep Cariaco Basin, the  $\delta^2\text{H-CH}_4$  and  $\delta^{13}\text{C-CH}_4$  values are isotopically much lighter than in the Black Sea. The difference in the extents of CH<sub>4</sub> oxidation between the deep Black Sea and Cariaco Basin is responsible for the differences in deep basin stable isotope values.

## 5. Conclusions

[43] Fluxes of CH<sub>4</sub> from seafloor seeps are emerging as significant contributors in global and oceanic carbon and CH<sub>4</sub> cycles [e.g., Judd, 2004; Sansone et al., 2001]. However, studying their biogeochemistry is difficult in an open ocean environment owing to advection, mixing, and dilution. The restricted circulation of large anoxic basins allows assembling CH<sub>4</sub> budgets, since CH<sub>4</sub> accumulates without open-ocean dispersion. The stable isotope results of CH<sub>4</sub> show large differences between the Black Sea and Cariaco Basin, despite the first-order similarities of the two environments. Radiocarbon results of CH<sub>4</sub> in the Black Sea and Cariaco Basin confirm that the dominant source of CH<sub>4</sub> to both of these basins is fossil and effectively balance both CH<sub>4</sub> budgets. Anaerobic oxidation of CH<sub>4</sub> rates, time series [CH<sub>4</sub>] analyses, and the radiocarbon results indicate that both basins are open systems (i.e., CH<sub>4</sub> is being added at the same time it is being oxidized) and that the Cariaco Basin is not in steady state. However, the  $\delta^{13}\text{C-CH}_4$  results suggest that the Black Sea is in steady state. Application of newly derived open-system stable isotope equations to both basins suggests that the Black Sea is in steady state and permits determination of the  $\alpha$  for AOM in a water column

environment and the stable isotope signature of CH<sub>4[S]</sub> released into the Cariaco Basin. Steady state conditions in the Black Sea are responsible for oxidizing CH<sub>4</sub> dissolved in the water column to a different extent than the non-steady-state conditions in the Cariaco Basin; the large differences in  $\delta^2\text{H-CH}_4$  and  $\delta^{13}\text{C-CH}_4$  between the deep basins are attributed to this kinetic isotope effect. The distributions of identified seeps provide an explanation why the stable isotope profiles are mirror images between the Black Sea and Cariaco Basin, as highlighted by a vertical box model for the stable isotopes of CH<sub>4</sub>.

[44] **Acknowledgments.** We thank the crews of the R/V *Knorr* and the B/O *Hermano Gines* for their support at sea, Ramon Varela and David Valentine for scientific support at sea, Richard Seifert for providing the Black Sea seep gas samples, Yrene Astor for her help with Cariaco Basin cruise and equipment coordination, and John Southon, Guaciara dos Santos, and Xiaomei Xu for laboratory support. We thank Max Wolfsberg for beneficial discussions on isotope modeling. This manuscript was improved by unusually thorough, meticulous, and constructive reviews by Marc Alperin, and we are grateful for his efforts. This work was supported by the National Science Foundation (grants OCE-0096280, OCE-0326928) and by instrumentation awards (IRMS and AMS) from the W. M. Keck Foundation.

## References

- Albert, D. B., C. Taylor, and C. S. Martens (1995), Sulfate reduction rates and low molecular weight fatty acid concentrations in the water column and surficial sediments of the Black Sea, *Deep Sea Res., Part I*, 42, 1239–1260.
- Alperin, M. J., W. S. Reeburgh, and M. J. Whiticar (1988), Carbon and hydrogen isotope fractionation resulting from anaerobic methane oxidation, *Global Biogeochem. Cycles*, 2(3), 279–288.
- Alptekin, Ö., J. L. Nábelek, and M. N. Toksöv (1986), Source mechanism of the Bartın Earthquake of September 3, 1968 in Northwestern Turkey: Evidence for active thrust faulting at the Southern Black Sea margin, *Tectonophysics*, 122, 73–88.
- Amouroux, D., G. Roberts, S. Rapsomanikis, and M. O. Andreae (2002), Biogenic Gas (CH<sub>4</sub>, N<sub>2</sub>O, DMS) emission to the atmosphere from near-shore and shelf waters of the north-western Black Sea, *Estuarine Coastal Shelf Sci.*, 54, 575–587.
- Astor, Y., F. Muller-Karger, and M. I. Scranton (2003), Seasonal and inter-annual variation in the hydrography of the Cariaco Basin: implications for basin ventilation, *Cont. Shelf Res.*, 23, 125–144.
- Atkinson, L. P., and F. A. Richards (1967), The occurrence and distribution of methane in the marine environment, *Deep Sea Res.*, 14, 673–684.
- Audemard, F. A., G. Romero, H. Rendon, and V. Cano (2005), Quaternary fault kinematics and stress tensors along the southern Caribbean from fault-slip data and focal mechanism solutions, *Earth Sci. Rev.*, 69, 181–233.
- Bernard, B. B., J. M. Brooks, and W. M. Sackett (1976), Natural gas seepage in the Gulf of Mexico, *Earth Planet. Sci. Lett.*, 31, 48–54.
- Bigeleisen, J., and M. Wolfsberg (1958), Theoretical and experimental aspects of isotope effects in chemical kinetics, *Adv. Chem. Phys.*, 1, 15–76.
- Clark, J. F., L. Washburn, J. S. Hornafius, and B. P. Luyendyk (2000), Dissolved hydrocarbon flux from natural marine seeps to the southern California Bight, *J. Geophys. Res.*, 105(C5), 11,509–11,522.
- Deuser, W. G. (1974), Evolution of anoxic conditions in Black Sea during Holocene, in *The Black Sea—Geology, Chemistry, and Biology*, edited by E. T. Degens and D. A. Ross, pp. 133–136, Am. Assoc. of Petrol. Geol., Tulsa, Okla.
- Dickens, G. R., and M. S. Quinby-Hunt (1994), Methane hydrate stability in seawater, *Geophys. Res. Lett.*, 21(19), 2115–2118.
- Dimitrov, L. (2002), Contribution to atmospheric methane by natural seepages on the Bulgarian continental shelf, *Cont. Shelf Res.*, 22, 2429–2442.
- Fanning, K. A., and M. E. Q. Pilson (1972), A model for the anoxic zone of the Cariaco Trench, *Deep Sea Res.*, 19, 847–863.
- Ginsburg, G. D., A. N. Kremlev, M. N. Grigor'ev, G. V. Larkin, A. D. Pavlenkin, and N. A. Satykova (1990), Filtrigenic gas hydrates in the Black Sea, *Geol. Geofiz.*, 31(3), 10–19.
- Grabowski, K. S., D. L. Knies, S. J. Tumey, J. W. Pohlman, C. S. Mitchell, and R. B. Coffin (2004), Carbon pool analysis of methane hydrate re-

- gions in the seafloor by accelerator mass spectrometry, *Nucl. Instrum. Methods Phys. Res., Sect. B*, 223–224, 435–440.
- Gulin, S. B., G. G. Polikarpov, and V. N. Egorov (2003), The age of microbial carbonate structures grown at methane seeps in the Black Sea with an implication of dating of the seeping methane, *Mar. Chem.*, 84, 67–72.
- Hoehler, T. M., M. J. Alperin, D. B. Albert, and C. S. Martens (1994), Field and laboratory studies of methane oxidation in an anoxic marine sediment: Evidence for a methanogen-sulfate reducer consortium, *Global Biogeochem. Cycles*, 8(4), 451–463.
- Hoehler, T. M., M. J. Alperin, D. B. Albert, and C. S. Martens (1998), Thermodynamic control on hydrogen concentrations in anoxic sediments, *Geochim. Cosmochim. Acta*, 62, 1745–1756.
- Holmén, K. J., and C. G. H. Rooth (1990), Ventilation of the Cariaco Trench, a case of multiple source competition?, *Deep Sea Res.*, 37, 203–225.
- Isakov, I. S. (Ed.) (1953), *Morskoi Atlas: Izdaniye Morskogo General'zhnogo Shtaba* (in Russian), vol. 2, 72 pp., Voenno-Morskoye Min. Soyuza SSR, Moscow.
- Ivanov, M. V., N. V. Pimenov, I. I. Rusanov, and A. Y. Lein (2002), Microbial processes of the methane cycle at the north-western shelf of the Black Sea, *Estuarine Coastal Shelf Sci.*, 54, 589–599.
- Iversen, N., and B. B. Jørgensen (1985), Anaerobic methane oxidation rates at the sulfate-methane transition in marine sediments from Kattegat and Skagerrak (Denmark), *Limnol. Oceanogr.*, 30(5), 944–955.
- Jones, G. A., and A. R. Gagnon (1994), Radiocarbon chronology of Black Sea sediments, *Deep Sea Res., Part I*, 41, 531–557.
- Jørgensen, B. B., A. Weber, and J. Zopf (2001), Sulfate reduction and anaerobic methane oxidation in Black Sea sediments, *Deep Sea Res., Part I*, 48, 2097–2120.
- Judd, A. G. (2004), Natural seabed gas seeps as sources of atmospheric methane, *Environ. Geol.*, 46, 988–996.
- Keeling, C. D. (1958), The concentration and isotopic abundances of atmospheric carbon dioxide in rural areas, *Geochim. Cosmochim. Acta*, 13, 322–334.
- Keeling, C. D. (1961), The concentration and isotopic abundances of carbon dioxide in rural and marine air, *Geochim. Cosmochim. Acta*, 24, 277–298.
- Kelley, D. S., et al. (2005), A serpentinite-hosted ecosystem: The Lost City hydrothermal field, *Science*, 307, 1428–1434.
- Kessler, J. D. (2005), Studies on oceanic methane: Concentrations, stable isotope ratios ( $\delta^2\text{H-CH}_4$ ,  $\delta^{13}\text{C-CH}_4$ ), and natural radiocarbon measurements ( $^{14}\text{C-CH}_4$ ), Ph.D. thesis, Univ. of Calif., Irvine.
- Kessler, J. D., and W. S. Reeburgh (2005), Preparation of natural methane samples for stable isotope and radiocarbon analysis, *Limnol. Oceanogr. Methods*, 3, 408–418.
- Kessler, J. D., W. S. Reeburgh, J. Southon, and R. Varela (2005), Fossil methane source dominates Cariaco Basin water column methane geochemistry, *Geophys. Res. Lett.*, 32, L12609, doi:10.1029/2005GL022984.
- Kessler, J. D., W. S. Reeburgh, J. Southon, R. Seifert, W. Michaelis, and S. C. Tyler (2006), Basin-wide estimates of the input of methane from seeps and clathrates to the Black Sea, *Earth Planet. Sci. Lett.*, 243, 366–375.
- Kutas, R. I., S. I. Paliy, and O. M. Rusakov (2004), Deep faults, heat flow and gas leakage in the northern Black Sea, *Geo Mar. Lett.*, 24, 163–168.
- Latif, M. A., E. Ozsoy, T. Oguz, and Ü. Ünlüata (1991), Observations of the Mediterranean inflow into the Black-Sea, *Deep Sea Res.*, 38, S711–S723.
- Leifer, I., J. R. Boles, B. P. Luyendyk, and J. F. Clark (2004), Transient discharges from marine hydrocarbon seeps: Spatial and temporal variability, *Environ. Geol.*, 46, 1038–1052.
- Lüdmann, T., H. K. Wong, P. Konerding, M. Zillmer, J. Petersen, and E. Flüh (2004), Heat flow and quantity of methane deduced from a gas hydrate field in the vicinity of the Dnieper Canyon, northwestern Black Sea, *Geo Mar. Lett.*, 24, 182–193.
- Luth, C., U. Luth, A. V. Gebruk, and H. Thiel (1999), Methane gas seeps along the oxic/anoxic gradient in the Black Sea: Manifestations, biogenic sediment compounds and preliminary results on benthic ecology, *Mar. Ecol.*, 20(3–4), 221–249.
- Maloney, N. J. (1966), Geomorphology of continental margin of Venezuela: Part I. Cariaco Basin, *Bol. Inst. Oceanogr.*, 5, 38–53.
- Martens, C. S., D. B. Albert, and M. J. Alperin (1999), Stable isotope tracing of anaerobic methane oxidation in gassy sediments of Eckernförde Bay, German Baltic Sea, *Am. J. Sci.*, 299, 589–610.
- Mendoza, C. (2000), Rupture history of the 1997 Cariaco, Venezuela, earthquake from teleseismic P waves, *Geophys. Res. Lett.*, 27(10), 1555–1558.
- Michaelis, W., et al. (2002), Microbial reefs in the Black Sea fueled by anaerobic oxidation of methane, *Science*, 297, 1013–1015.
- Pape, T., R. Seifert, M. Blumenberg, K. Peterknecht, V. Thiel, O. Schmale, J. Sultenfub, and W. Michaelis (2003), Seep gases, dissolved carbon compounds and noble gases at the Ukrainian Shelf (Black Sea), in *EGS-AGU-EUG Joint Assembly*, edited by G. R. Abstracts, p. EAE03-A-14658, Eur. Geophys. Soc., Nice, France.
- Pataki, D. E., J. R. Ehleringer, L. B. Flanagan, D. Yakir, D. R. Bowling, C. J. Still, N. Buchmann, J. O. Kaplan, and J. A. Berry (2003), The application and interpretation of Keeling plots in terrestrial carbon cycle research, *Global Biogeochem. Cycles*, 17(1), 1022, doi:10.1029/2001GB001850.
- Peterson, L. C., G. H. Haug, R. W. Murray, K. M. Yarinicik, J. W. King, T. J. Bralower, K. Kameo, S. D. Rutherford, and R. B. Pearce (2000), Late Quaternary stratigraphy and sedimentation at site 1002, Cariaco Basin (Venezuela), *Proc. Ocean Drill. Program Sci. Results*, 165, 85–99.
- Reeburgh, W. S. (1976), Methane consumption in Cariaco Trench waters and sediments, *Earth Planet. Sci. Lett.*, 28, 337–344.
- Reeburgh, W. S. (1980), Anaerobic methane oxidation: Rate depth distributions in Skan Bay sediments, *Earth Planet. Sci. Lett.*, 47, 345–352.
- Reeburgh, W. S. (2003), Global methane biogeochemistry, in *Treatise on Geochemistry*, edited by H. D. Holland and K. K. Turekian, pp. 65–89, Elsevier, New York.
- Reeburgh, W. S., B. B. Ward, S. C. Whalen, K. A. Sandbeck, K. A. Kilpatrick, and L. J. Kerkhof (1991), Black Sea methane geochemistry, *Deep Sea Res.*, 38, S1189–S1210.
- Reeburgh, W. S., S. C. Tyler, and J. B. Carroll (2006), Stable carbon and hydrogen isotope measurements on Black Sea water column methane, *Deep Sea Res., Part II*, 53, 1893–1900.
- Richards, F. A., and R. F. Vaccaro (1956), The Cariaco Trench, an anaerobic basin in the Caribbean Sea, *Deep Sea Res.*, 3, 214–228.
- Robinson, A. G., J. H. Rudat, C. J. Banks, and R. L. F. Wiles (1996), Petroleum geology of the Black Sea, *Mar. Pet. Geol.*, 13(2), 195–223.
- Ross, D. A., E. Uchupi, K. E. Prada, and J. C. MacIvaine (1974), Bathymetry and microtopography of Black Sea, in *The Black Sea—Geology, Chemistry, and Biology*, edited by E. T. Degens and D. A. Ross, pp. 1–10, Am. Assoc. of Pet. Geol., Tulsa, Okla.
- Sansone, F. J., B. N. Popp, A. Gasc, A. W. Graham, and T. M. Rust (2001), Highly elevated methane in the eastern tropical North Pacific and associated isotopically enriched fluxes to the atmosphere, *Geophys. Res. Lett.*, 28(24), 4567–4570.
- Sassen, R., S. T. Sweet, A. V. Milkov, D. A. DeFreitas, and M. C. Kennicutt II (2001), Thermogenic vent gas and gas hydrate in the Gulf of Mexico slope: Is gas hydrate decomposition significant?, *Geology*, 29(2), 107–110.
- Scranton, M. I. (1977), The marine geochemistry of methane, Ph.D. thesis, Woods Hole Oceanogr. Inst., Woods Hole, Mass.
- Scranton, M. I. (1988), Temporal variations in the methane content of the Cariaco Trench, *Deep Sea Res.*, 35, 1511–1523.
- Scranton, M. I., F. L. Sayles, M. P. Bacon, and P. G. Brewer (1987), Temporal changes in the hydrography and chemistry of the Cariaco Trench, *Deep Sea Res.*, 34, 945–963.
- Scranton, M. I., Y. Astor, R. Bohrer, T.-Y. Ho, and F. Muller-Karger (2001), Controls on temporal variability of the geochemistry of the deep Cariaco Basin, *Deep Sea Res., Part I*, 48, 1605–1625.
- Stuiver, M., and H. A. Polach (1977), Discussion: Reporting  $^{14}\text{C}$  data, *Radiocarbon*, 19(3), 355–363.
- Suárez, G., and J. Nábelek (1990), The 1967 Caracas earthquake: Fault geometry, direction of rupture propagation and seismotectonic implications, *J. Geophys. Res.*, 95(B11), 17,459–17,474.
- Tans, P. P. (1997), A note on isotopic ratios and the global atmospheric methane budget, *Global Biogeochem. Cycles*, 11(1), 77–81.
- Thunell, R., E. Tappa, R. Varela, M. Llano, Y. Astor, F. Muller-Karger, and R. Bohrer (1999), Increased marine sediment suspension and fluxes following an earthquake, *Nature*, 398, 233–236.
- Valentine, D. L., D. C. Blanton, W. S. Reeburgh, and M. Kastner (2001), Water column methane oxidation adjacent to an area of active hydrate dissociation, Eel River Basin, *Geochim. Cosmochim. Acta*, 65, 2633–2640.
- Vassilev, A., and L. Dimitrov (2002), Spatial and quantity evaluation of the Black Sea gas hydrates, *Russ. Geol. Geophys.*, 43(7), 672–684.
- Ward, B. B., K. A. Kilpatrick, P. C. Novelli, and M. I. Scranton (1987), Methane oxidation and methane fluxes in the ocean surface layer and deep anoxic waters, *Nature*, 327, 226–229.
- Wiesenburg, D. A. (1975), Processes controlling the distribution of methane in the Cariaco Trench, Venezuela, M.S. thesis, Old Dominion Univ., Norfolk, Va.

- Winckler, G., W. Aeschbach-Hertig, J. Holocher, R. Kipfer, I. Levin, C. Poss, G. Rehder, E. Suess, and P. Schlosser (2002a), Noble gases and radiocarbon in natural gas hydrates, *Geophys. Res. Lett.*, 29(10), 1423, doi:10.1029/2001GL014013.
- Winckler, G., W. Aeschbach-Hertig, J. Holocher, R. Kipfer, I. Levin, C. Poss, G. Rehder, E. Suess, and P. Schlosser (2002b), Correction to “Noble gases and radiocarbon in natural gas hydrates”, *Geophys. Res. Lett.*, 29(15), 1735, doi:10.1029/2002GL015735.
- Yamamoto, S., J. B. Alcauskas, and T. E. Crozier (1976), Solubility of methane in distilled water and seawater, *J. Chem. Eng. Data*, 21(1), 78–80.
- Zonenshain, L. P., and X. L. Pichon (1986), Deep basins of the Black Sea and Caspian Sea as remnants of Mesozoic back-arc basins, *Tectonophysics*, 123, 181–211.

---

J. D. Kessler, Department of Geosciences, Princeton University, Princeton, NJ 08544-1003, USA. (jdkessle@princeton.edu)

W. S. Reeburgh and S. C. Tyler, Department of Earth System Science, University of California, Irvine, Irvine, CA 92697-3100, USA.